PREPARATION, PHASE FORMATION AND STRUCTURE STUDY
OF Mn BASED ALLOYS

I. Janotová, P. Švec Sr., P. Švec, I. Maťko, D. Janičkovič, M. Mihalkovič

Institute of Physics, Slovak Academy of Sciences, Bratislava, Slovakia,
irena.janotova@savba.sk

1. Introduction

Because of their attractive magnetic properties [1,2] manganese based compounds are a promising new platform for design of new advanced permanent magnets and are one of the targets in search for magnetic materials that can replace rare-earth-based alloys with more abundant and less strategically important elements. Pure manganese has a large unit cell containing different sites, where Mn atoms bear magnetic moments which order into a noncollinear antiferromagnetic structure [1,2,3]. This ability of Mn to carry large magnetic moment is known for more than 70 years. The problem is to find a combination of elements and tune the structure by thermal treatment to achieving sufficiently high moment with ferromagnetic order in a dense-packed structure [1]. However, due to the difficulty in preparing pure polycrystalline specimens, many of the fundamental physical properties have never been "unambiguously" determined; therefore, literature states difference in properties and structure depending on the preparation and processing techniques.

AlMn/MnBi particles could be established as the next generation of particulate media used in magnetic recording devices. These systems are interesting as a perspective alternative to conventional high-strength rare-earth based magnets applied e.g. in magnetic information storage systems [1-5]. Magnetic properties are determined by the existence (formation) of ferromagnetic τ-MnAl phase [1,4-6] or low-temperature phase (LTP) α-MnBi [1,2,7], which exhibit high coercivity and saturation magnetization [1,4-6], low density and good corrosion resistance coupled with low cost of constituent elements. Magnetic properties of Mn-based systems are sensitive to the microstructure and the presence of defects developed during the ferromagnetic phase formation and these attributes are strongly determined by the nature of production route employed [2,4-8]. Ferromagnetic phases are strongly influenced by the starting composition (Mn:Al or/and Mn:Bi ratio) and exist between 45-55 at % Mn[1-4].

Formation of pure metastable ferromagnetic τ-phase with tetragonal superstructure can be achieved in Al-Mn system by multiple viable routes, among them by rapid quenching of the parent high temperature hexagonal close packed (hcp) ε-phase, followed by suitable isothermal annealing or by controlled cooling [3-5]. The phase diagram in Fig. 1 (left) shows that the transformation - two-step reaction process of ε into τ phase - can take place by different mechanisms depending on the microstructure and purity of the ε phase. One of the approaches is to pass from the parent hexagonal (A3) ε-MnAl phase through the intermediate B19-structured ε'-phase followed by isothermal annealing at temperatures in the range 623–923 K. Occurrence of the intermediate phases (described in Table 1) depends on thermal treatment. It has been reported that this transformation is controlled by diffusional nucleation and growth processes [4-6] leading to formation of metastable tetragonal τ-MnAl phase designated as L1_0 type (similar to CuAu type) or as tetragonal phase (tP2) [3-6], which is the only magnetic phase of AlMn. The process is referred to as "massive" transformation preferentially occurring at the grain boundaries of the ε phase. The formation of the τ-phase

has also been reported to be accompanied by micro-twinning associated with stress relaxation at the growth front [6].
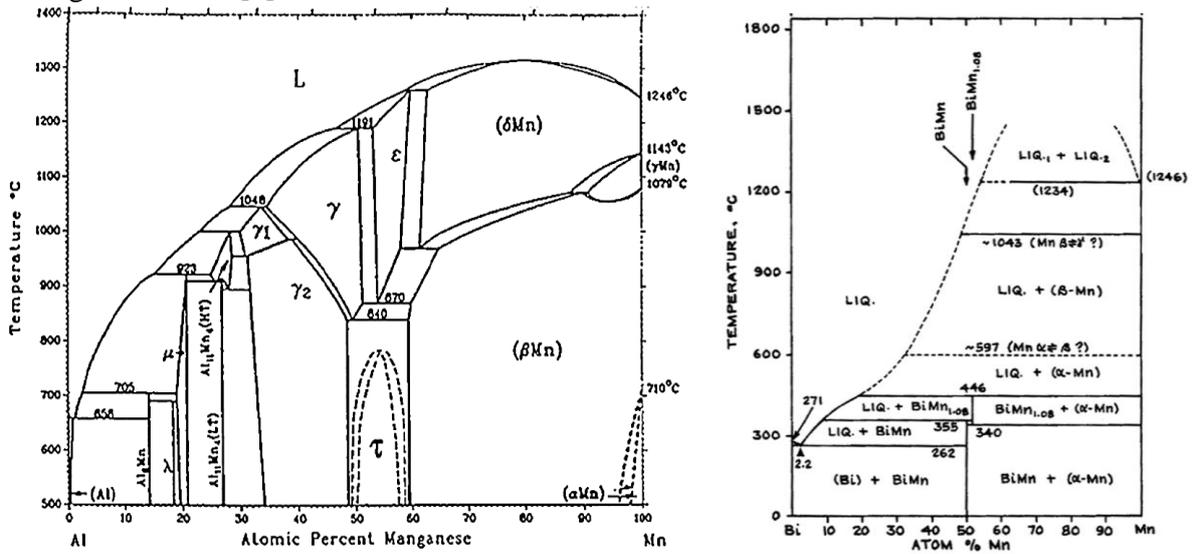
Fig. 1: *Phase diagrams of the binary Al-Mn (left) [9] and Bi-Mn (right) [10] systems.*

Table 1. *Selected characteristics of the phases occurring in the Al-Mn phase diagram in the vicinity of the τ-MnAl structure.*

Phase	Struc.	S. group	Cell parameters (Å)			Mag. moment
			a	*b*	*c*	
α-Mn	Cub.	I-43m	8,912	-	-	Paramag.
τ-MnAl	Tetrag.	tP2/L1$_0$ P4/mmm	3.94	-	3.58	Ferromag.
ε-MnAl	Hex.	A3 P63/mmc	2.69	-	4.38	Paramag.
ε´-MnAl	Ortho.	B19	3,006	≈ a	≈ a	Paramag.

Table 2. *Selected characteristics of the phases occurring in the Bi-Mn phase diagram in the vicinity of the α-MnBi structure.*

Phase	name	Struc.	S. group	Cell parameters (Å)			Mag. moment
				a	*b*	*c*	
α-Mn	-	Cub.	I-43m	8,912	-	-	Paramag.
Bi	-	Hex.	P6$_3$/mmc	4,537	-	5,200	Diamag.
α-MnBi	LTP	Hex.	P6$_3$/mmc	4,29	-	6,126	Ferromag.
α -MnBi	NP	Hex.	P6$_3$/mmc	4,32	-	5,83	Ferrimag.
β-MnBi	HTP	Hex.	P6$_3$/mmc	4,38	-	6,00	Paramag.
β-MnBi	QHTP	Hex.def	P6$_3$/mmc	4,34	-	5,97	Ferromag.

As can be seen in the **Mn-Bi** phase diagram (Fig. 1 right), formation of the ferromagnetic LTP α-MnBi phase is more complicated. The ferromagnetic phase is formed as a result of two

reactions, a peritectic reaction (1′ at 719 K) where Bi rich liquid and Mn react into β-MnBi and Bi rich liquid, followed by the next peritectic reaction (2′ at 628 K) where Bi rich liquid and β-MnBi transform to α-MnBi and Bi rich liquid and further into solid Bi and α-MnBi in an eutectic reaction at 538K [7,8,10-12]. This liquid-phase separation is used in the preparation technology.

Several closely related forms of the equiatomic intermetallic compound MnBi with hexagonal structure and similar cell parameters [6,10-11] exist. As shown in Table 2 the lattice parameters have significant influence on the magnetic moment. The α-MnBi formation from β-MnBi is accompanied by a slight volume decrease (0,1%) due to position change of 10-15% Mn.

2. Experimental details

Mn based samples in form of ribbon 3 mm wide and ~ 17 μm thick were prepared by planar flow casting (PFC) method. The ribbons were cast from master alloy manufactured in induction furnace from elemental components with purity better than 99.95% (electrolytic) under Ar atmosphere. $Al_{45}Mn_{55}$ ribbon could by prepared by this technique without any protective atmosphere by ejection of the melt onto the cooper wheel. BiMn ribbon had been prepared in special PFC chamber in protective Ar atmosphere. The structures of the master alloy, as–cast and isothermally annealed samples were investigated by X-ray diffraction (XRD) using Bruker D8 Advance diffractometer (CuKα radiation). Phase transformations were investigated using differential scanning calorimetry (DSC 7 Perkin Elmer, Ar atmosphere, heating rate 10 K/min), especially to determine the temperatures of transformation onset (T_x). Curie temperature (T_c) of the formed magnetic phase was determined by magnetic thermogravimetry (TGA7 Perkin Elmer, Ar atmosphere, heating rate 10K/min) with small external magnet. Annealing parameters were selected from DSC and TGA measurements, samples were isothermally annealed in vacuum.

3. Results and discussion

The transformation behavior from as quenched state during linear heating was studied by thermal analysis techniques (DSC, TGA). DSC traces (Fig. 2) show different demeanor for the two investigated Mn based systems. Only a single transformation from ε-AlMn to τ-AlMn was observed in the Al-Mn sample. The temperature of the transformation onset T_x is close to 700 K. The same thermal regime in Bi-Mn sample leads to series of transformations. The broad exotherm in the range 400-430 K is probably a consequence of atomic reorganization in the α-MnBi hexagonal structure from ferrimagnetic NP to ferromagnetic LTP (Table 2). The three endothermic peaks on the normalized heat flow curve are in good correlation with the phase diagram (Fig. 1). The first endothermic reaction at 535 K is a result of α-MnBi + Bi solid becoming α-MnBi + Bi rich liquid, similar to eutectic transformation. This is followed by two peritectic transformations at higher temperatures – at 629 K the phase αMnBi changed to β-MnBi and at 720 K the disintegration of βMnBi to α-Mn + Bi rich liquid took place. The height of the peaks (and the "area under the peaks") in the second heating run is visibly changed. In the eutectic transformation the peak is higher because of the separation of the MnBi phase into Mn + Bi. The peritectic transformations of MnBi are irreversible; the content of the phases entering the transformations is decreased, having been consumed during the first run and therefore the magnitude of the corresponding peaks is nearly zero.

DSC measurements were used to find the temperature range of formation of metastable ferromagnetic phases, i.e. the parameters for controlled head treatment used to achieve the highest content of ferromagnetic phase. TGA measurements of the annealed AlMn and BiMn samples during subsequent linear heating (10K/min) are shown in Fig. 3.

Curie temperatures for the AlMn sample T_c = 635 K +/- 0,5 K and for the BiMn sample T_c = 645 K +/- 0,5 K were estimated from the decrease of magnetic weight of the sample annealed for 1 hour during its subsequent heating after cooling to room temperature.
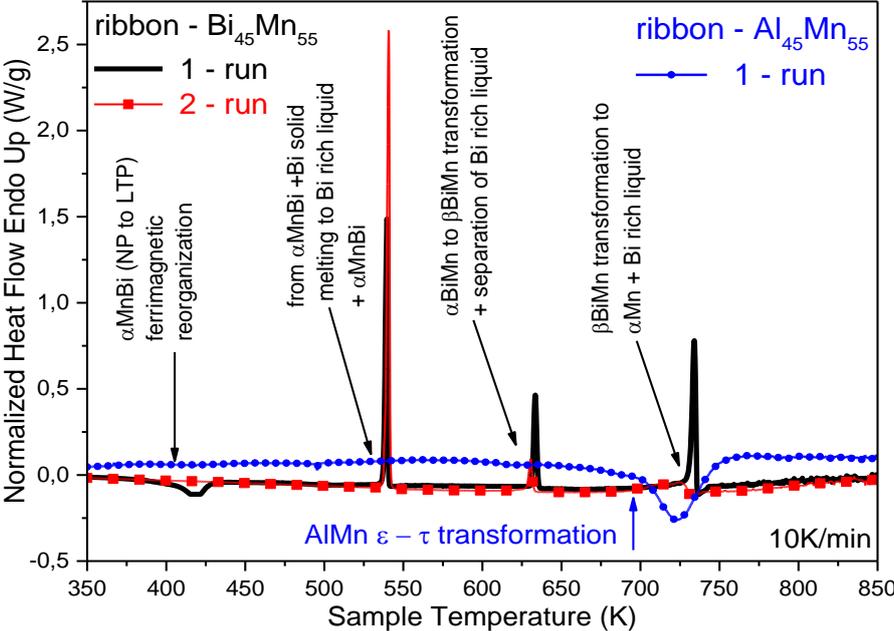
Fig. 2: *DSC traces of as-quenched Al₄₅Mn₅₅ and BiMn ribbons.*
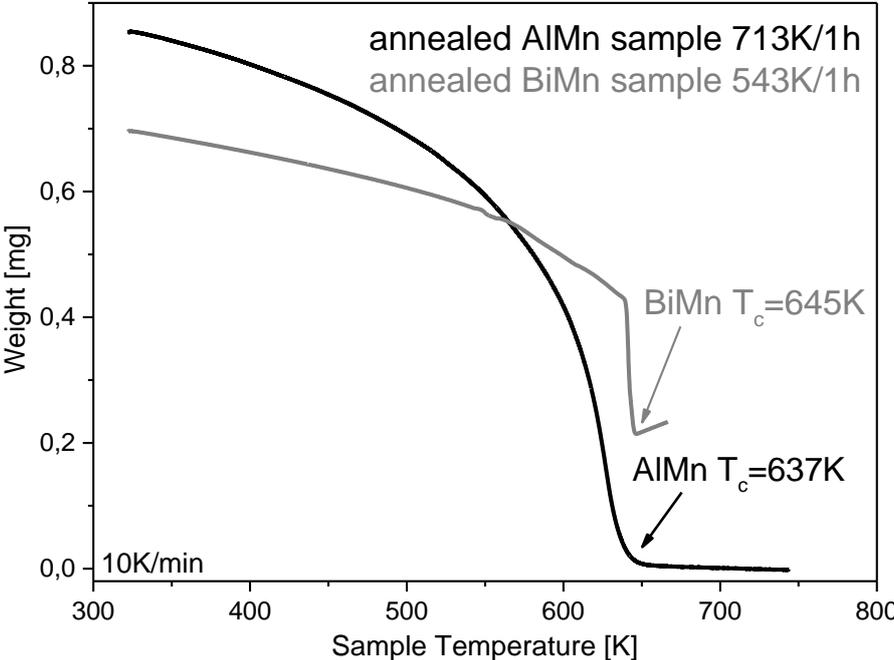
Fig. 3: *TGA curves measured on annealed AlMn and BiMn ribbons, T_c is identified by sharp weight decrease.*

The AlMn based sample was isothermally annealed at 673 K for 1 hour and at 713 K for 1 and 12 hours. Phase analysis of various heat-treated Al₄₅Mn₅₅ samples by XRD is shown

in Fig. 4a. The comparison of these XRD patterns allows to follow the structure changes from nonmagnetic as cast state - nearly monophase hexagonal ε-AlMn (hP2) to the transformation – (rearrangement) of Mn-rich phases. Annealed samples exhibit the presence of ferromagnetic τ-AlMn tetragonal (L1$_0$: tP2) phase. The master alloy contained a mixture of phases together with a certain amount of tetragonal τ – AlMn magnetic phase (with small grain sizes).
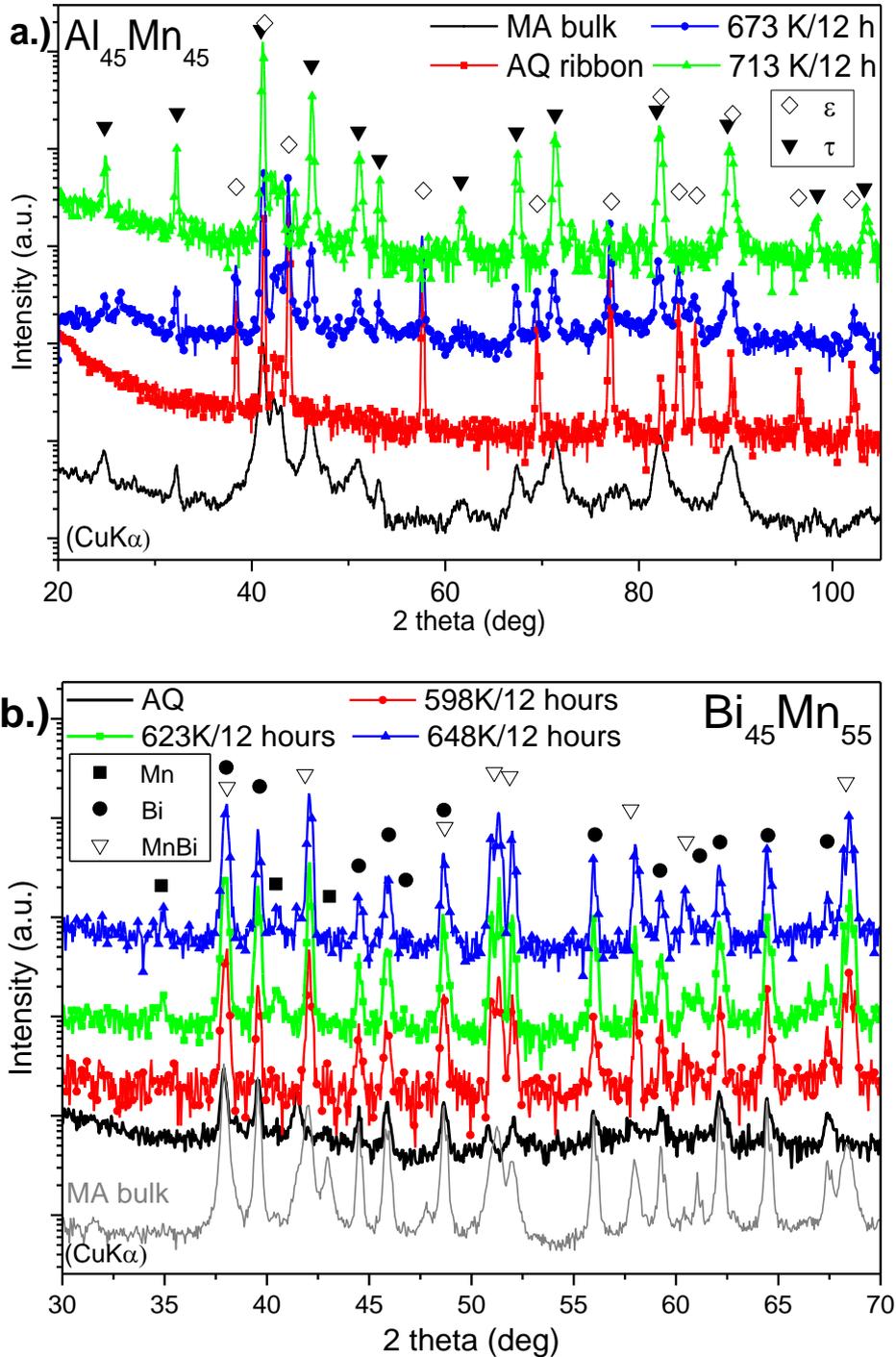
Fig. 4: *XRD patterns of Al$_{45}$Mn$_{55}$(a.) and Bi$_{45}$Mn$_{55}$ (b.) sample in different states and heat treatment - evolution of ferromagnetic phases due the preparation from master alloy from which a ribbon was cast and isothermally annealed at specific temperatures.*

From this analysis it can be seen that the sample annealed by 713 K exhibits fully the content of this magnetic phase - monophased expense of $L1_0$ phase, which is dominant in the as-cast structure [13]. This measurement proved the transformation of hexagonal ε-AlMn after annealing at higher temperature and sufficient time to tetragonal τ-AlMn. The comparison of two different annealing regimes shows that the temperatures of isothermal annealing should lie above 700 K.

X-ray diffraction patterns of investigated BiMn sample in form of master alloy (MA), as- cast ribbons (AQ) and ribbons after different annealing regimes are shown in Fig. 4b. The Bi and Mn content changed at the expense on MnBi phase, which can be identified also in the MA and AQ samples. The detected patterns from annealed ribbons and phase analysis clearly shows the increase of Mn and Bi content in samples heated at 623 and 648 K for 12 hours, what is in accord with the results from DSC measurements. Sample annealed for the same time at 598 K exhibits just a small change in Mn and Bi content and contained about 60 vol.% of the LTP αMnBi. The lattice parameters of the different hexagonal $P6_3/mmc$ MnBi phases, however, could not be determined with sufficient accuracy by this technique because of overlapping of diffraction peaks and similar cell parameters.

4. Conclusion

The Al-Mn and Bi-Mn based thin ribbons were prepared by rapid quenching. The effect of alloying of constituting elements (in ratio about 1/1) on the changes of physical properties caused by structural transformations was studied. The samples were annealed with different regimes to obtain the desired structure possessing sufficient magnetic anisotropy. The selected processing conditions allowed to obtain a nearly monophase structure containing τ-AlMn phase with reasonably high maximum energy product. The maximal content of LTP αMnBi in BiMn sample achieved using the presented processing methods was around 60 vol.%.

References
[1]   Y. Nagata, H. Sano, K. Ohta, *Jap. J. Appl. Phys.* **23** (1984) 580-584.
[2]   J. M. D. Coey, J. Phys.: *Condens. Matter* **26** (2014) 064211.
[3]   C. Yanar, et al.; *Metallurgical and Materials Transactions* **33A**, (2002) 2413-2423.
[4]   F. J. Villacorta et al.; *Metals* **4** (2014), 8-19.
[5]   N. Singh, et al.; *Journal of Alloys and Compounds* **633** (2015) 401–407.
[6]   A.V. Dobromyslov et al.; *Phys. Stat. Sol.* **A 88** (1985) 443-454.
[7]   T. Chen, W. E. Stutius, *IEEE Transactions on Magnetics* **10** (1974) 581-586.
[8]   K. Oikawa, Y. Mitsui, K. Koyama, K. Anzai, *Mat. Trans.* **52** (2011) 2032-2039.
[9]   T.B. Massalski; Binnary Alloy Phase Diagrams, TMS, Materials Park OH (1990).
[10] P.-K. Nguyen, S. Jin, A. E. Berkowitz, *IEEE Transactions on Magnetics* **49** (2013) 3387-3390.
[11] X. Guo, A. Zaluska, Z. Altounian, J. O. Strom-Olsen, *J. Mater. Res.* **5** (1990) 2646-2651.
[12] T. Chen, *J. Appl. Phys.* **45** (1974) 2358-2360.
[13] I. Janotova, P. Svec Sr., P. Svec, I. Matko, D. Janickovic, J. Zigo, M. Mihalkovic, J. Marcin, I. I. Skorvanek, *Journal of Alloys and Compounds* **707** (2017) 137-141.